Received: 6 May 2022 | Revised: 16 September 2022 | Accepted: 19 September 2022

DOI: 10.1002/alz.12825

Alzheimer's & Dementia®
THE JOURNAL OF THE ALZHEIMER'S ASSOCIATION

RESEARCH ARTICLE

Identification of causal effects of neuroanatomy on cognitive decline requires modeling unobserved confounders

Sebastian Pölsterl[1] | **Christian Wachinger**[1,2] | **the Alzheimer's Disease Neuroimaging Initiative**[†] | **the Japanese Alzheimer's Disease Neuroimaging Initiative**[‡]

[1]The Lab for Artificial Intelligence in Medical Imaging (AI-Med), Department of Child and Adolescent Psychiatry, Ludwig-Maximilians-Universität, Munich, Germany

[2]Technical University of Munich, School of Medicine, Department of Radiology, Munich, Germany

Correspondence
Sebastian Pölsterl, The Lab for Artificial Intelligence in Medical Imaging (AI-Med), Department of Child and Adolescent Psychiatry, Ludwig-Maximilians-Universität, Nussbaumstraße 5, 80336 Munich, Germany.
Email: sebastian.poelsterl@med.uni-muenchen.de

[†]Data used in the preparation of this article were obtained from the Alzheimer's Disease Neuroimaging Initiative (ADNI) database (adni.loni.usc.edu). As such, the investigators within the ADNI contributed to the design and implementation of ADNI or provided data but did not participate in the analysis or writing of this report. A complete listing of ADNI investigators can be found at http://adni.loni.usc.edu/wp-content/uploads/how_to_apply/ADNI_Acknowledgement_List.pdf.

[‡]Data used in the preparation of this article were obtained from the Japanese Alzheimer's Disease Neuroimaging Initiative (J-ADNI) database deposited in the National Bioscience Database Center Human Database, Japan (Research ID: hum0043.v1, 2016). As such, the investigators within J-ADNI contributed to the design and implementation of J-ADNI or provided data but did not participate in the analysis or writing of this report. A complete listing of J-ADNI investigators can be found at https://humandbs.biosciencedbc.jp/en/hum0043-j-adni-authors.

Funding information
National Institutes of Health, Grant/Award Number: U01 AG024904; Department of Defense Award, Grant/Award Number:

Abstract

Introduction: Carrying out a randomized controlled trial to estimate the causal effects of regional brain atrophy due to Alzheimer's disease (AD) is impossible. Instead, we must estimate causal effects from observational data. However, this generally requires knowing and having recorded all confounders, which is often unrealistic.

Methods: We provide an approach that leverages the dependencies among multiple neuroanatomical measures to estimate causal effects from observational neuroimaging data without the need to know and record all confounders.

Results: Our analyses of $N = 732$ subjects from the Alzheimer's Disease Neuroimaging Initiative demonstrate that using our approach results in biologically meaningful conclusions, whereas ignoring unobserved confounding yields results that conflict with established knowledge on cognitive decline due to AD.

Discussion: The findings provide evidence that the impact of unobserved confounding can be substantial. To ensure trustworthy scientific insights, future AD research can account for unobserved confounding via the proposed approach.

Alzheimer's & Dementia®
THE JOURNAL OF THE ALZHEIMER'S ASSOCIATION

W81XWH-12-2-0012; Federal Ministry of Education and Research, Grant/Award Number: 031L0200A; Bavarian State Ministry of Science and the Arts

1 | BACKGROUND

During the last decade, a number of data-sharing initiatives have been established in neuroimaging that make it possible to identify disease predictors with low effect sizes. However, despite efforts to standardize data collection, confounding is a major concern that limits the ability of large-scale neuroimaging studies to uncover markers with a true cause-and-effect relationship. Often, the relationship between a marker and an outcome is confounded because there are one or more latent factors that are a common cause of both the marker and the outcome.[1] In the worst case, the observed association is only due to the latent confounder(s), and there is no direct causal link between the marker and the outcome. An important aspect of confounding is that, whether it is present depends on the research question being studied. For instance, age is often considered a confounder in studies on Alzheimer's disease (AD), but if the study focuses on age-related cognitive decline in a healthy population, age is not considered a confounder.[2] Therefore, it is vital to rigorously define the research question and the causal quantities in which one is interested. If the study is subject to confounding, investigators need to account for it. Otherwise, they risk drawing erroneous conclusions because the collected data will be compatible with many – potentially contradictory – causal explanations that cannot be distinguished from each other based on the data alone.[1]

Previous work on confounding in neuroimaging mostly assumed that all confounding variables were known and had been measured. In the Regress-Out approach, volume and thickness measurements are replaced by the residuals of a regression model fitted to estimate the original volume/thickness from the confounding variables.[3–9] A second stream of work adjusts for confounders via instance weights that are used in a downstream classification or regression model to obtain a pseudo-population that is approximately balanced with respect to the confounders.[10,11] Note that both the Regress-Out and weighting approaches could lead to valid causal estimates if all confounders are accounted for, but none of the previously cited work actually studied whether causal effects could be identified.

Our previous investigation across 17 neuroimaging studies revealed that considerable bias remained in volume and thickness measurements after adjusting for age, gender, and type of MRI scanner.[12] In addition, a study on confounders in the UK Biobank brain imaging study identified hundreds of potential confounders related just to the acquisition process.[13] These results suggest that having records on all confounders is an unrealistic assumption. Instead, we must acknowledge the presence of unobserved confounding effects. Studies using Mendelian randomization (MR) are based on a strong theoretical foundation from causal inference to account for unobserved confounders.[14–21] Their downside is that they require the selection of an instrumental variable that is causal only for the measurement of interest but not the unobserved confounder, which cannot be verified based on data alone. MR addresses this issue by searching for a single-nucleotide polymorphism (SNP) as the instrumental variable, such that the SNP is believed to be causal only for the measurement of interest. Finding a suitable SNP can be challenging because most SNPs will have pleiotropic effects, for example, due to alternative splicing, and thus influence the phenotype of interest as well as other factors that affect the outcome of interest. This would violate the assumption that the SNP only influences the outcome via the phenotype of interest. Multivariable MR overcomes this by explicitly modeling pleiotropy.[22] In addition, SNPs are often in linkage disequilibrium with each other, which makes it hard to establish that a specific SNP is indeed causal for the phenotype of interest and not another SNP that is in linkage disequilibrium with it.[23]

The aim of this study was to estimate casual effects of regional brain atrophy on cognition in the AD continuum. In our analyses, we explicitly acknowledge the existence of unobserved confounding and apply a recently developed statistical method to estimate a substitute confounder from regional volume and thickness measurements.[24] When applied to data from the Alzheimer's Disease Neuroimaging Initiative (ADNI), our results demonstrate that ignoring unobserved confounding leads to conclusions that are misleading and not in agreement with our current understanding of AD. When accounting for unobserved confounding, those misconceptions are resolved and one arrives at biologically meaningful conclusions. Our replication study on data from the Japanese ADNI (J-ADNI) provides further evidence that the impact of unobserved confounding is substantial and that it can be overcome with the proposed approach to obtain a trustworthy diagnostic model.

2 | METHODS

2.1 | Data

We used T1-weighted magnetic resonance imaging (MRI) brain scans from the baseline visit of $N = 732$ subjects with an Alzheimer's pathologic change (CSF $A\beta_{42} \leq 192$ pg/ml;[25]) from ADNI.[26] In our replication study, we used MRI from baseline visits of $N = 101$ subjects with Alzheimer's pathology (CSF $A\beta_{42} \leq 333$ pg/ml; [27]) from the J-ADNI.[28] The characteristics of the datasets are summarized in Table 1.

Each scan was segmented with FreeSurfer[29] to obtain cortical thickness and subcortical volume measurements. We combined measurements from the left and right hemispheres and averaged highly correlated thickness measurements belonging to the same lobe. This resulted in 11 subcortical volume measurements and 20 cortical thickness measurements. The distribution of each measurement was normalized to appear normally distributed (Appendix A.1).

RESEARCH IN CONTEXT

1. **Systematic review**: The authors reviewed the literature using traditional sources that focused on confounding and causal inference in neuroimaging studies. Previous research did not discuss whether causal effects were identifiable from observational data.
2. **Interpretation**: This article studied the impact of confounding on estimating the causal effects of regional brain atrophy on cognition in the Alzheimer's disease continuum. We found that ignoring unobserved confounding could lead to conclusions that conflicted with our current understanding of cognitive impairment due to Alzheimer's disease. Therefore, we propose to account for unobserved confounding by estimating a substitute confounder, which resolves those misconceptions.
3. **Future directions**: As neuroimaging studies continue to increase in size, the potential impact of unobserved confounding is expected to increase. Future research should explicitly consider unobserved confounders and discuss their consequences in their study.

2.2 | Causal inference

Having observed data on $D = 31$ neuroanatomical measures $X_1, \ldots, X_D$ and the associated Alzheimer's Disease Assessment Scale Cognitive Subscale 13 score (ADAS;[30]), we want to estimate the average change in ADAS in a hypothetical experiment in which we modify the brains of subjects such that the volumes/thicknesses of neuroanatomical structures in S have the values $x'_S \in \mathbb{R}^{|S|}$:

$$\mathbb{E}[\text{ADAS}|do(X_S = x'_S)]. \quad (1)$$

The expectation is called the average causal effect (ACE), and the conditioning operator $do(\cdot)$ denotes an intervention that sets the neuroanatomical measures X_S equal to x'_S.[1]

The central question in causal inference is that of identification: Is the ACE uniquely determined by the observed joint distribution over volume/thickness measures and the ADAS? Usually, this is only the case if we know and record all confounders, that is, all common causes of neuroanatomy and the ADAS. The causal graph in Figure 1A captures the known relationships in AD that are associated with our research question and highlights the quantities of interest in red (see Appendix A.2 for details on its construction). From the graph we can conclude that there are two sources that confound the relationship between neuroanatomy and ADAS: (i) age as a known confounder,[31] and (ii) U as a representative of all other factors that previous research highlighted but are unmeasured and unknown.[12, 13] Therefore, it appears that unobserved confounding (due to U) prevents us from uniquely identifying the ACE of neuroanatomy on cognition from observational data (Appendix A.3).

TABLE 1 Characteristics of data from Alzheimer's Disease Neuroimaging Initiative (ADNI) and Japanese ADNI (J-ADNI) used in this study. ATN classification is not available for J-ADNI

	ADNI (N=732)	J-ADNI (N=101)
Age		
Mean (SD)	73.82 (7.13)	72.34 (6.02)
Range	54.40 – 91.40	60.98 - 83.68
Gender		
Female	324 (44.3%)	51 (50.5%)
Male	408 (55.7%)	50 (49.5%)
Education		
≤ 12 years	121 (16.5%)	45 (44.6%)
12–16 years	322 (44.0%)	52 (51.5%)
> 16 years	289 (39.5%)	4 (4.0%)
ATN classification[71]		
A+/T-/N-	92 (12.6%)	–
A+/T+/N-	256 (35.0%)	–
A+/T+/N+	384 (52.5%)	–
ADAS-Cog 13		
Mean (SD)	19.58 (9.99)	22.71 (7.846)
Range	1.00 – 55.00	4.00 - 44.00

2.3 | Estimating a substitute confounder

In general, unobserved confounding prevents us from estimating causal effects from observational data.[1] Our proposed approach, based on the work of Wang and Blei,[24] overcomes the identifiability issue by making assumptions on the data generation process. In particular, we assume that the unobserved confounder U causally affects multiple (≥ 2) neuroanatomical structures. In other words, we assume that there is no unobserved confounder that only affects a single structure. This assumption is plausible because common sources of confounding, such as scanner, protocol, and aging, affect the brain as a whole and not just individual regions.[32, 33] Based on this assumption, the key insight of our proposed method is that the neuroanatomical structures $X_1, \ldots, X_D$ we are interested in become conditionally independent given the unobserved confounder U and their observed causes $PA_{X_1,\ldots,X_D}$, which includes the observed confounder age:

$$P(x_1, \cdots, x_D|U, PA_{X_1,\cdots,X_D}) = \prod_{d=1}^{D} P(x_d|U, PA_{X_1,\cdots,X_D}). \quad (2)$$

Therefore, we can obtain a substitute confounder $\mathbf{z} \in \mathbb{R}^K$ for the unobserved confounder U by estimating the conditional distribution with a probabilistic latent factor model (PLFM). Here, we estimate a substitute confounder using probabilistic principal component analysis (PPCA;[34]) and Bayesian Probabilistic Matrix Factorization (BPMF;[35]) using PyStan 2.19.1.1[36] (Appendices A.4 and A.5).

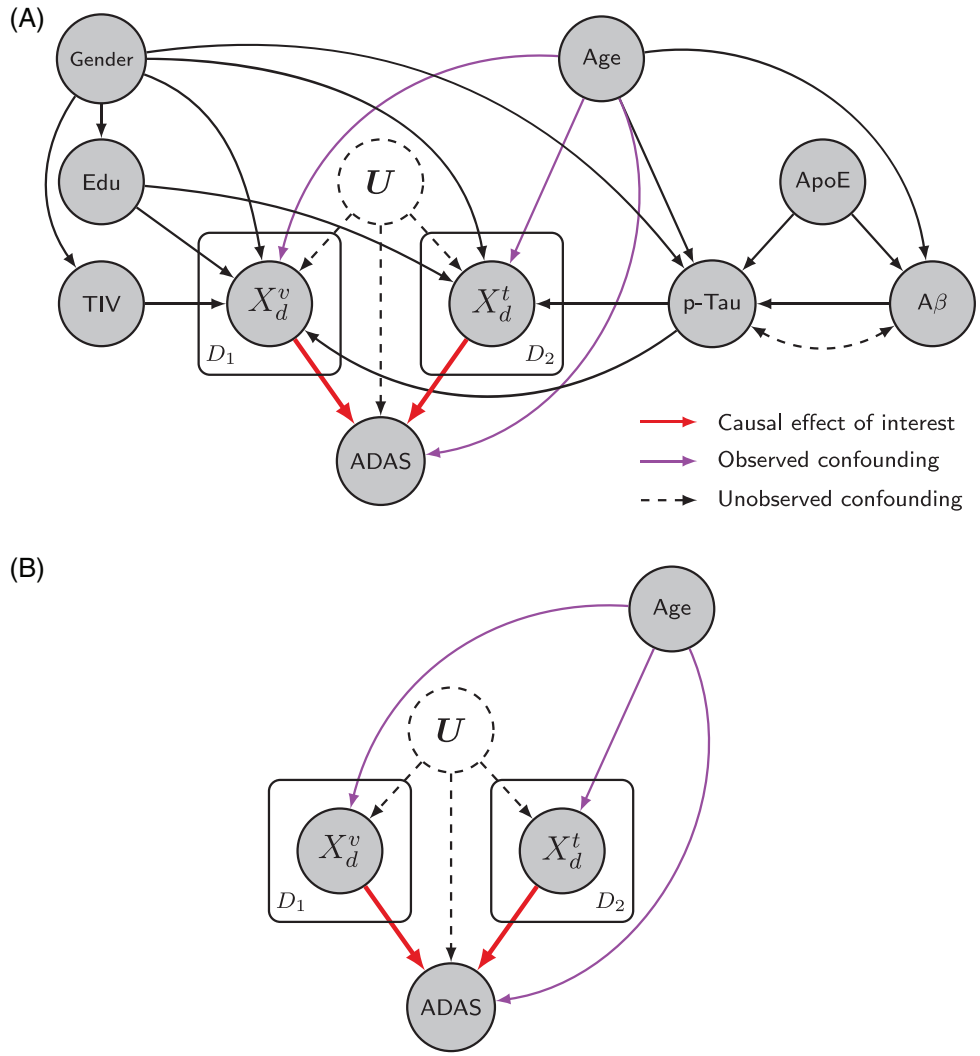

FIGURE 1 **(A)** Causal graph used to estimate the causal effect (red arrow) of subcortical volumes ($X_d^v; d = 1, \ldots, D_1$) and cortical thicknesses ($X_d^t; d = 1, \ldots, D_2$) on cognitive function (ADAS) in the presence of an unknown and unobserved confounder U. Exogenous variables irrelevant for estimating the causal effect of interest are not shown. Circles are random variables and arrows causal relationships. Filled circles are observed, transparent circles are hidden, bidirectional edges denote unobserved common causes. **(B)** Variables required to identify the causal effect of neuroanatomical measurements X_d^v, X_d^t on the ADAS (see Appendix A.6 for the proof).

2.4 | Identifiability of causal effects

When it is proven that the latent representation of any PLFM does indeed render the relationship between neuroanatomical measures and ADAS unconfounded (Appendix A.6), the ACE of a subset of neuroanatomical measures S can be estimated from observational data by accounting for the variables in Figure 1B. Effectively, we must fit a model to predict the ADAS from neuroanatomical measures, age, and the substitute confounder. Since the ADAS ranges between 0 and 85 (higher values indicate a more pronounced cognitive impairment), we convert it to proportions in the interval (0, 1) and use a Bayesian beta regression model[37] as implemented in rstanarm 2.19.3[36]. We account for collinear features using a normal prior on the regression coefficients (Appendix A.7).

2.5 | Comparative analysis

We estimated the causal effect of 11 subcortical volume measurements and 20 cortical thickness measurement on the ADAS-Cog 13 (Figure 2). We compare our approach of estimating causal effects with three non-causal alternatives: (i) ignoring all observed and unobserved confounders (Non-Causal), (ii) only accounting for the observed confounder age via residualization (Regress-Out;[3]), and (iii) removing scanner effects across 60 ADNI sites with ComBat.[4] For the latter, we preserve biological variability due to the causes of neuroanatomical measures in Figure 1A that are not confounders: years of education, gender, and p-Tau. All models have access to the same set of 31 neuroanatomical measurements and only differ in the set of confounders they account for. Hence, we use the Non-Causal model to illustrate

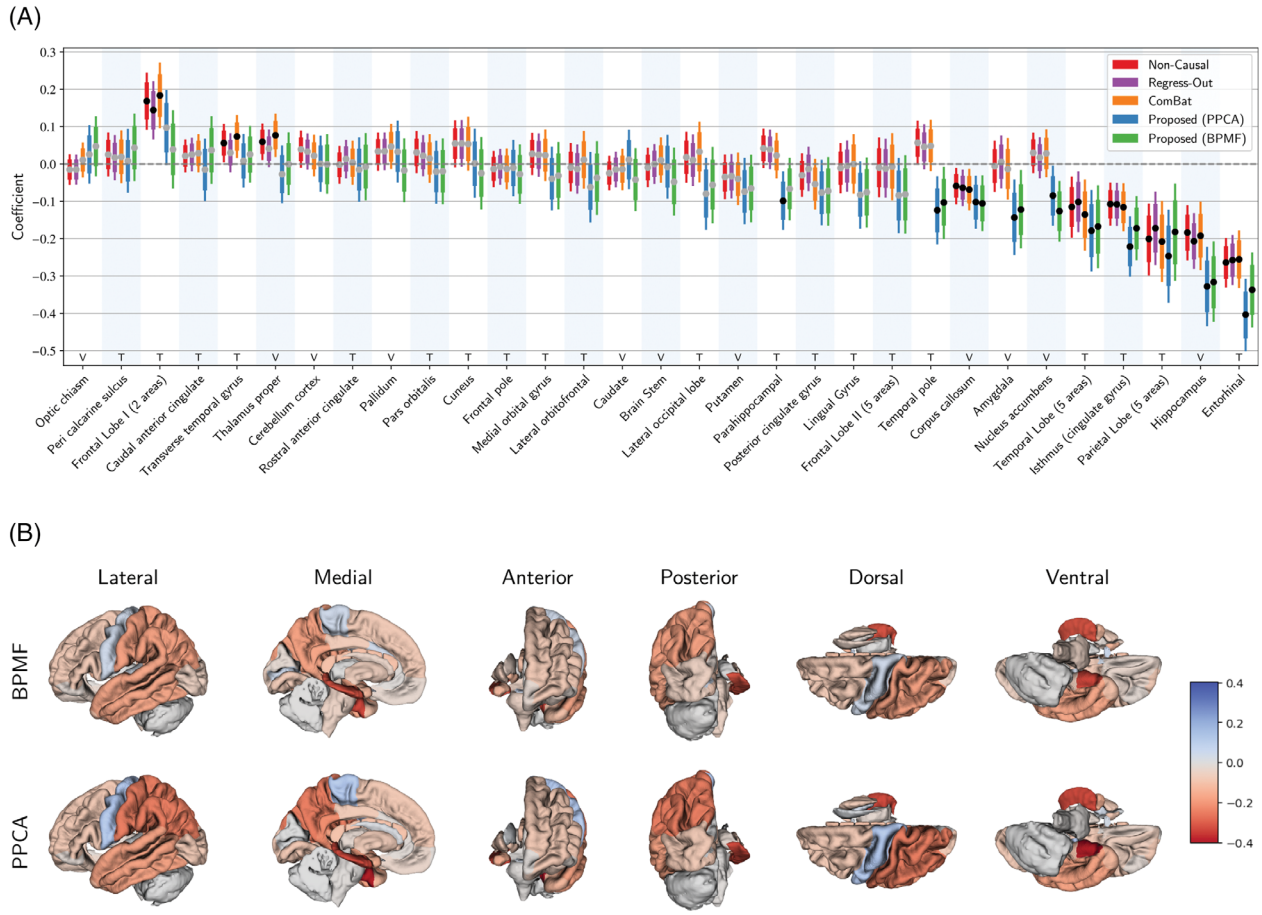

FIGURE 2 Estimated coefficients on data from ADNI. **(A)** Mean coefficient (dot), 80% (thick line), and 95% (thin line) credible interval of volume and thickness measures. Significant effects are marked with a black dot. The proposed approach uses six substitute confounders. See Appendix C for 1–8 substitute confounders. **(B)** Anatomical view of mean coefficients when estimating a substitute confounder via BPMF and PPCA

the consequences if one is oblivious to all types of confounding, the Regress-Out model to illustrate the consequences of only accounting for the observed confounder age, and ComBat to investigate the impact of harmonization across scanners and sites. We consider an effect to be statistically significant if the 95% credible interval (CI; thin line) does not contain zero. A CI is analogous to a confidence interval in frequentist statistics but considers the parameter to be random and not the bounds of the interval. Hence, the 95% CI of a parameter provides the interval that contains the true parameter with a probability of 95%.

3 | RESULTS

3.1 | Quantitative evaluation

Note that the true causal effect strengths are unknown and we must rely on a qualitative comparison. For a quantitative evaluation, we performed experiments on brain MRI from the UK Biobank with synthetically generated outcomes, as described in Appendix B. Briefly, these results show that accounting for unobserved confounding does reduce the bias in estimated effect strengths considerably and that our proposed approach is robust to the choice of PLFM and number of substitute confounders.

3.2 | Estimation of causal effects in ADNI

For four out of 31 brain structures, estimates are statistically significant when accounting for unobserved confounding via a substitute confounder, whereas they are insignificant for the Non-Causal and Regress-Out approaches: nucleus accumbens volume, amygdala volume, parahippocampal thickness, and temporal pole thickness. In addition, three measures are deemed statistically significant by the Non-Causal, Regress-Out, and ComBat approaches but insignificant after accounting for unobserved confounding: frontal lobe I thickness (paracentral lobule, precentral gyrus), transverse temporal gyrus thickness, and thalamus proper volume. For the remaining measures, statistical significance does not change, but the estimated effect strength can differ substantially.

The six biggest absolute differences with respect to the Non-Causal mean estimate are consistent across PPCA and BPMF approaches:

thickness of temporal pole, parahippocampus and entorhinal cortex, and volume of hippocampus, amygdala, and nucleus accumbens. For parahippocampal and temporal lobe thickness and volumes of nucleus accumbens and amygdala, the 80% CIs (thick lines) do not overlap, which supports the idea that the effect strength is significantly underestimated when unobserved confounding is ignored.

We can also observe that mean estimates of seven structures go from positive to negative after unobserved confounding is accounted for: volumes of thalamus proper and nucleus accumbens, and thickness of pars orbitalis, medial orbital gyrus, lateral occipital lobe, parahippocampus, and temporal pole. Among these, nucleus accumbens volume and thickness of parahippocampus and temporal pole stand out because their estimates flip the sign and go from statistically insignificant to significant. That means that atrophy of these structures is insignificantly associated with cognitive improvement in the Non-Causal and Regress-Out approaches (positive mean coefficient, CIs contain zero), but atrophy is a significant cause of cognitive decline according to the proposed causal models (negative mean coefficient, CIs exclude zero).

A change from negative to positive mean estimates can be observed for optic chiasm and caudate, albeit at a smaller scale – their CIs continue to cover zero. Finally, the meta-ROI frontal lobe I has a positive coefficient across all methods, which indicates that an increase in thickness is linked to cognitive decline. However, this effect is only statistically significant when ignoring unobserved confounding (Non-Causal, Regress-Out, ComBat).

Although the ACE is fully parameterized by the coefficients in Figure 2A, Figure 3 shows the estimated ACE across varying interventions for structures with a statistically significant effect strength. Note that we used a linear model for the estimation of causal effects, but its link function is non-linear, and non-linear transformations have been applied to the measurements (Appendix A.1). Therefore, the ACE can be non-linear with respect to neuroanatomical measures. The figure shows that accounting for the observed confounder age, but ignoring unobserved confounding, only results in a minor difference, compared to ignoring all confounders. Similarly, harmonizing measurements with ComBat changes very little. When observed and unobserved confounding is accounted for, differences are much more pronounced.

When comparing the results obtained by estimating a substitute confounder via PPCA vs. BPMF, the differences are comparatively small. The biggest differences occur at the extremes of the distribution of measurements. When considering the ACE at the center of the distribution (between the first and third quartile), estimates differ only slightly. The biggest difference is 1.6 for frontal lobe I at the third quartile, which is much smaller than the difference to the Non-Causal and Regress-Out estimates (4.3–6.1). When estimating the ACE at the mean of the corresponding measurement, differences between the Regress-Out approach and the proposed approach range between 3.73 (hippocampus) and 6.78 (frontal lobe I) with a mean difference of 5.1 across all structures. The bias due to unobserved confounding increases when intervening on multiple structures. As an example, let us consider the composite ACE of setting the measurements of the 11 ROIs in Figure 3A from the median to the lower quartile ($\mathbb{E}[\text{ADAS}|do(x_{25})] - \mathbb{E}[\text{ADAS}|do(x_{50})]$) as depicted in Figure 3B. When ignoring unobserved confounding, this will lead to an estimated increase in the ADAS of 7.5 (Non-Causal), 7.7 (Regress-Out), and 8.3 (ComBat), whereas when unobserved confounding is accounted for the increase is estimated to be 19.7 (PPCA) and 18.3 (BPMF).

3.3 | Replication study in J-ADNI

To investigate whether our conclusions derived on data from ADNI are generalizable, we repeated our experiments on 101 subjects from J-ADNI (Table 1). Note that we could not evaluate ComBat because J-ADNI does not disclose identifiers of clinical sites.

Owing to the small sample size of the J-ADNI data, the causal effects of only three structures reach statistical significance (Figure 4A and Appendix D). Atrophy of the hippocampus and entorhinal cortex has been estimated to have the largest impact on cognition (most negative mean coefficient), which matches our results on ADNI. However, the effect of atrophy of the entorhinal cortex is marginally insignificant when estimating substitute confounders via BPMF. When comparing mean estimates of the Non-Causal and Regress-Out models to the proposed models, the biggest differences are due to hippocampus volume, which is also among the biggest changes on ADNI (Figure 2A). Parahippocampus thickness is deemed a significant effect for both BPMF and PPCA on J-ADNI but is only significant with PPCA on ADNI. Nevertheless, when accounting for unobserved confounding, the estimate undergoes a change similar to that seen on ADNI, such that 80% CIs do not overlap. Although they are deemed statistically insignificant, we want to highlight results for temporal pole thickness. In both ADNI and J-ADNI, its mean estimate flips signs from positive to negative, such that atrophy is associated with cognitive improvement in the Non-Causal and Regress-Out models but with cognitive decline in the proposed models.

When considering the estimated ACE in Figure 4B, our conclusions from ADNI are confirmed. First, accounting for the observed confounder age affects estimates only marginally. Second, differences between the BPMF and PPCA models are minor and occur at the extremes of the observed distribution of volume and thickness measurements. Finally, the impact of ignoring unobserved confounding becomes most evident when considering the composite ACE of all statistically significant causes of the ADAS in Figure 4C. When accounting for unobserved confounding, the estimated effect on the ADAS is an increase of 10.2 (BPMF) and 10.5 (PPCA) points, whereas ignoring unobserved confounding will underestimate the effect (Non-Causal: 3.5; Regress-Out: 3.6).

4 | DISCUSSION

The results presented in the preceding section indicate that we arrive at strikingly different conclusions when ignoring unobserved

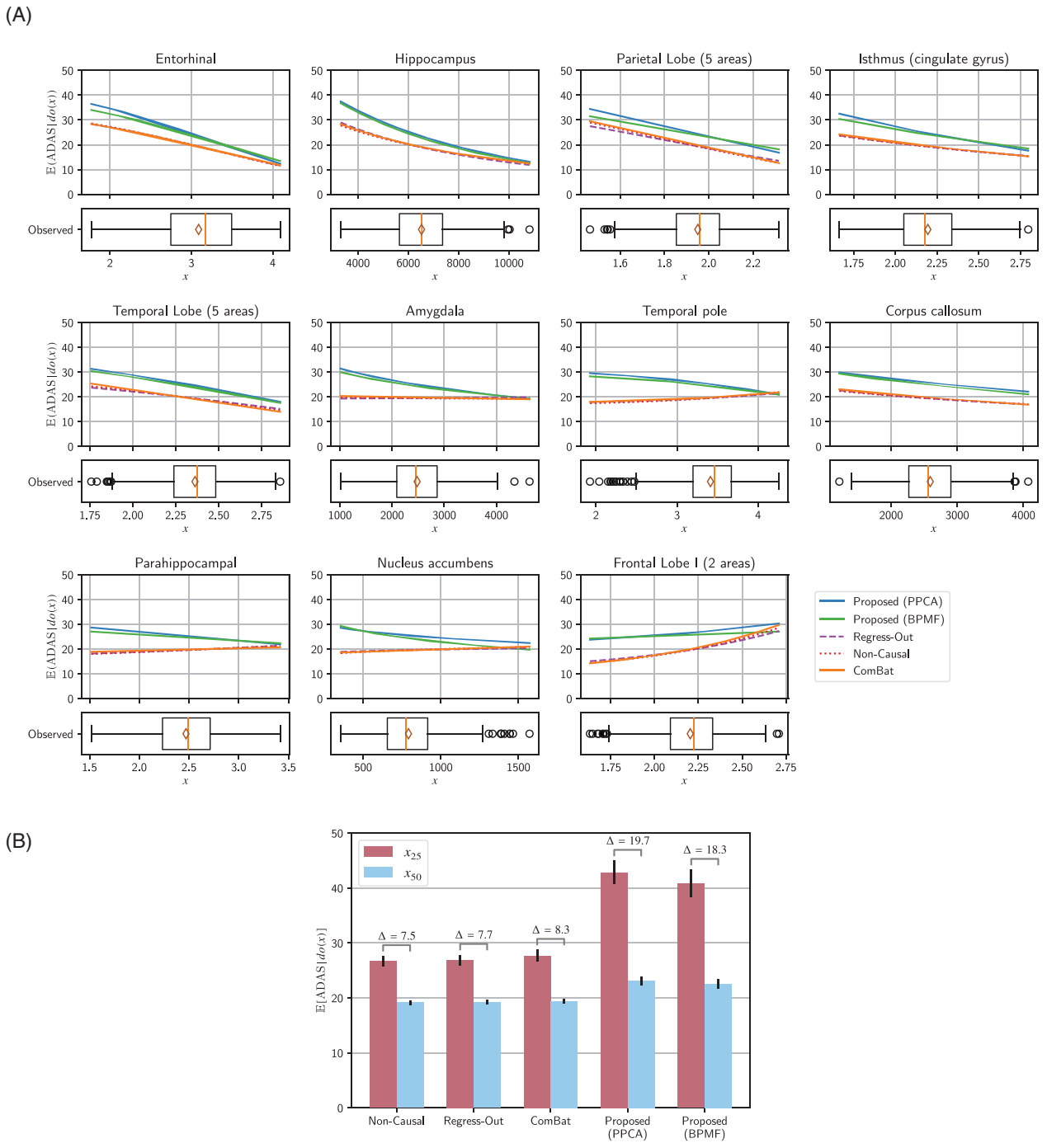

FIGURE 3 **(A)** Estimates of average causal effect (ACE) $\mathbb{E}[\text{ADAS}|do(x)]$ across structures with significant effect (Figure 2A). Note that the noncausal and regress-out approaches are by definition not valid estimators of the ACE because they ignore unobserved confounding. Box plots depict the distribution of volume/thickness measures in the observed data. Orange lines: median; diamonds: mean. **(B)** Composite ACE from setting the 11 structures in subfigure A from the median (x_{50}) to the lower quartile (x_{25})

confounding. Next, we will discuss these results in terms of our current understanding of cognitive decline in AD.

On ADNI, all models agree on the five regions that have the largest absolute mean coefficient. The most important causes of cognitive decline are entorhinal and hippocampal atrophy. This is a reassuring result because neural losses of the entorhinal cortex and hippocampus are among the best studied neuroimaging markers in AD.[38–41]

The third ranked cause of cognitive decline is parietal lobe atrophy. Although it is not considered a marker for traditional AD, it is a well-described pattern in the atypical presentation of posterior cortical atrophy (PCA; [42]). In subjects with AD of the PCA subtype, first symptoms are typically related to visual impairment rather than episodic memory impairment. Since the ADAS [30] assesses both aspects, and it is known that the ADNI study includes subjects with PCA,[43] the results

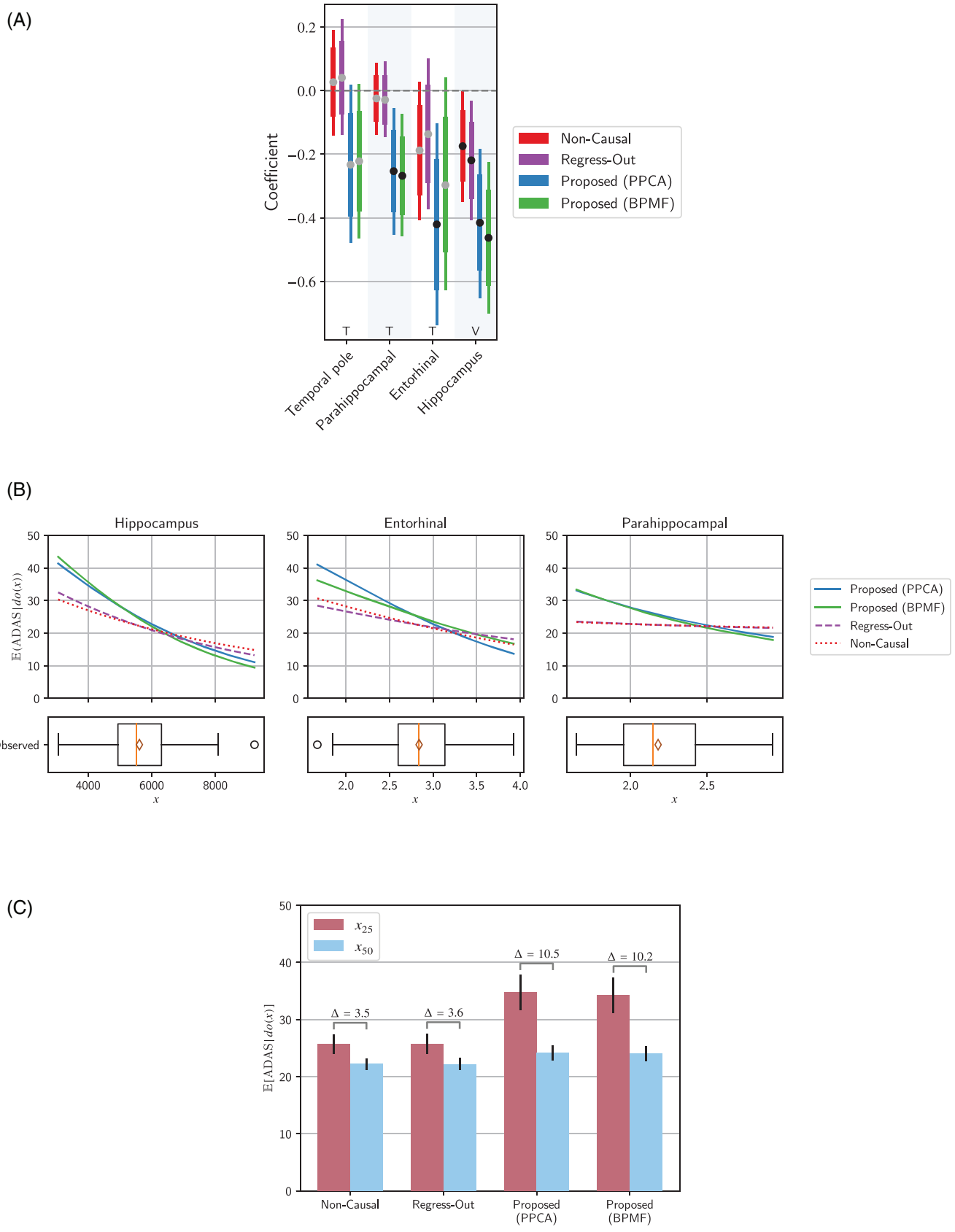

FIGURE 4 Selection of causal effects on J-ADNI. **(A)** Mean coefficient (dot), 80% (thick line), and 95% (thin line) credible interval of volume and thickness measures. Significant effects are marked with a black dot. The proposed approach uses six substitute confounders. See Appendix D for full results. **(B)** Estimates of average causal effect (ACE) $\mathbb{E}[\text{ADAS}|do(x)]$. **(C)** Composite ACE from setting the three structures in subfigure B from the median (x_{50}) to the lower quartile (x_{25}).

illustrate that the proposed approach can correctly capture cognitive decline across AD subtypes. Atrophy of the meta-ROI temporal lobe and isthmus of cingulate gyrus completes the top five most important causes. Atrophy of the temporal lobe, comprising fusiform, banks of superior temporal sulcus, superior temporal, inferior temporal, and middle temporal gyrus, is an established marker of AD and is known to affect cognitive function,[41, 44, 45] as confirmed by our results. Furthermore, atrophy of the isthmus of cingulate gyrus is a cause of cognitive decline, which agrees with the results of a study on cognition in prodromal AD[46] and on patterns of regional atrophy in subjects with mild cognitive impairment.[47]

We obtained strikingly different results when ignoring unobserved confounders for parahippocampal thickness, amygdala volume, nucleus accumbens volume, and temporal pole thickness. Parahippocampal thickness and amygdala volume are deemed statistically insignificant causes of cognition in the Non-Causal and Regress-Out models but statistically significant causes when accounting for unobserved confounding via the proposed approach. Both structures are part of the medial temporal lobe, whose function is critical in forming short-term memory. Neural loss in the parahippocampus and amygdala occurs early in the course of AD; hence, these areas are established markers for diagnosing AD.[38, 41, 48, 49] This effect is only captured correctly when accounting for unobserved confounding, as indicated by a negative mean coefficient. If it is ignored, unobserved confounding will cause the investigator to arrive at implausible conclusions that conflict with our current understanding of AD.

Although statistically insignificant, the results of the Non-Causal, Regress-Out, and ComBat models that atrophy of the nucleus accumbens leads to cognitive improvement (indicated by a positive mean coefficient) contradict previous research too. The nucleus accumbens integrates information from the limbic system and is a part of the ventral striatum, which is involved in regulating episodic memory function.[50] Previous researchers observed that atrophy of the nucleus accumbens correlates with cognitive impairment.[51, 52] This would only be captured correctly when accounting for unobserved confounding.

Similarly, the results for temporal pole thickness are statistically insignificant, but deceiving. Thinning of the temporal pole is associated with cognitive improvement in the non-causal models, but cognitive decline when unobserved confounding is accounted for. The results of models that ignore unobserved confounding again contradict previous results demonstrating that thinning correlates with AD and cognitive decline.[44, 53] Our analysis suggests that temporal pole thinning is a statistically significant cause of cognitive impairment, which has been verified by a recent MR study on the causal effects of cortical measures on AD.[20]

The result that atrophy of corpus callosum is causal of cognitive decline seems to be plausible, too (all models agree on this). The corpus callosum is the brain's largest white matter structure, integrating information from the left and right cerebral hemispheres. Several studies found corpus callosum atrophy in AD patients and its association with cognitive impairment.[54–57]

The results for the meta-ROI frontal lobe I are inconclusive. It has a statistically significant positive coefficient for the Non-Causal, Regress-Out, and ComBat approaches, meaning that models agree that thinning of this area leads to improved cognition. When accounting for unobserved confounding via PPCA, the estimated effect strength is slightly reduced and becomes barely insignificant. When using the BPMF approach, the effect is further reduced, such that the estimated 80% CI covers zero. Anatomically, the precentral gyrus and paracentral lobule comprise the primary motor cortex.[58]

Although AD pathology can be detected in the primary motor cortex of AD patients,[59] and animal models,[60] the underlying processes connecting atrophy of the primary motor cortex, motor deficits, and cognition remain unknown.[61] Previous research showed that atrophy of the primary motor cortex occurred in later stages of the disease, which may inhibit motor function.[61, 62] Ongoing efforts that focus on studying the association of cognitive and motor impairments might help to shed light on this aspect of AD.[63]

When the differences in estimated ACE in Figure 3 are considered, the consequences of ignoring confounding appear striking. Accounting only for observed confounding due to age changes the estimated effects nominally. Moreover, harmonizing data to account for scanner effects is ineffective with respect to addressing unobserved confounding. In contrast, when observed and unobserved confounding is accounted for via the proposed approach, conclusions can change drastically.

When considering interventions across multiple structures in Figure 3B, the bias due to unobserved confounding increases. Using the Non-Causal, Regress-Out, and ComBat models, the ACE is estimated to be 7.5, 7.7, and 8.3, respectively. However, when accounting for unobserved confounding, the increase is estimated to be 19.7 (PPCA) and 18.3 (BPMF). The ADNI study reported differences in the ADAS in the range 5–10 between diagnostic groups,[64, 65] which roughly corresponds to the difference when unobserved confounding is ignored (10.0 –12.2). Hence, it is likely that estimates made using a diagnostic model that ignores unobserved confounding would be misleading. This example clearly illustrates that one must account for unobserved confounding to obtain a trustworthy diagnostic model.

Our replication study on J-ADNI yielded only three statistically significant causes of the ADAS because the CIs are relatively large due to the limited sample size of 101 subjects. The results on J-ADNI confirm our results on ADNI that atrophy of the hippocampus and entorhinal cortex has the greatest impact on reducing cognitive abilities. It also confirms that ignoring unobserved confounding will result in estimates that underestimate the effect of atrophy on the ADAS by a large margin (Figure 4). Overall, we can conclude that the proposed approach is effective at correcting for unobserved confounding but that we can only detect the most significant factors in the ADAS with statistical significance. We believe a replication study on a dataset with a larger sample size would help to confirm factors with smaller effect sizes, too.

Despite the ability of the proposed approach to estimate causal effects in the presence of unobserved confounding, it does rely on important assumptions. The gold standard in estimating causal effects would be a randomized experiment, where subjects' cortical thicknesses and subcortical volumes are randomly assigned. Because this

is impossible, we must resort to an observational study. This requires several assumptions, some of which cannot be verified based on data alone. An alternative approach to estimating causal effects in the presence of unobserved confounding is MR. Like our approach, it requires making specific assumptions regarding causal relationships to render causal effects identifiable. MR assumes an instrumental variable – a SNP – that only influences the outcome via the neuroanatomical measure of interest, not through other paths. Considering that most SNPs have pleiotropic effects, finding a marker that satisfies this requirement is difficult, in particular, when we are interested in estimating the effects of many neuroanatomical structures.

Multivariable MR[22] allows estimation in the presence of pleiotropy but still requires that the majority of SNPs be valid instruments.[66] In contrast, the proposed approach requires that the unobserved confounder affects multiple (≥ 2) neuroanatomical structures. This provides us with information on the unobserved confounder such that we can estimate a substitute for it via a PLFM. When the aim of a study is to estimate the causal effects of many neuroanatomical structures, we believe that the assumptions of the proposed approach will be easier to satisfy than those of MR. Nevertheless, a multivariable MR study on the causal effects of 14 gray matter volumes on AD diagnosis identified the hippocampus and inferior temporal cortex, which aligns with our results.

Specifically, our approach is based on the following assumptions. First, it is inherently linked to the structure of the graph in Figure 1. This implies that we assume that the unobserved confounder is shared across two or more neuroanatomical measures and that there are no direct causal relationships between measurements. Unfortunately, both cannot be verified based on data, but we believe that likely candidates for the unknown confounder are scanner- or age-related, which would affect the brain as a whole and satisfy the first assumption. The second assumption that measurements are not causally dependent is plausible for cross-sectional data, too. Although brain regions are certainly connected, we argue that it is reasonable to assume that one structure's volume/thickness is not causal for another structure's volume/thickness, but both are the result of a higher-order biological process, which would satisfy this assumption. To account for cognitive reserve, we used years of education, but alternatives exist. We evaluated the American National Adult Reading Test[67] in Appendix E, which yielded comparable results. In this study, we assumed that gender had no effect on ADAS, but no consensus has been reached regarding whether this is truly the case.[68–70] However, accounting for gender as an additional observed confounder is made straightforward by including it in the beta regression model.

Another assumption is implied in the use of a linear model to estimate causal effects. Since there are infinitely many causal interventions on volume/thickness measures one could investigate, nonparametrical estimation becomes impossible, and we must resort to modeling. We did not consider interaction effects, but we did consider non-linear effects by transforming measurements (Appendix A.1). Because the true functional form of the effect of neuroanatomical measures on the ADAS is unknown, our model might be misspecified, which would introduce bias. This warrants further investigation into alternative approaches to modeling the causal effects of neuroanatomical measures on the ADAS.

In conclusion, causal analysis of neuroanatomy offers the possibility of estimating how cognition might change if we introduced a certain pattern of regional brain atrophy. This could help us improve our understanding about the neuroanatomical determinants of cognitive decline. Our analyses of the causal effects on cognition in the ADNI and J-ADNI studies demonstrated that this represents a daunting task because the impact of unobserved confounding is substantial, which renders causal effects unidentifiable. We overcame this challenge by estimating a substitute confounder via a latent factor model.

Our results on ADNI revealed that the causes of cognitive decline are atrophy of the entorhinal cortex, hippocampus, parietal lobe, isthmus of cingulate gyrus, the meta-ROI temporal lobe, amygdala, temporal pole, corpus callosum, nucleus accumbens, and parahippocampus.

If unobserved confounding is ignored, one risks arriving at conclusions that are misleading and in conflict with our current understanding of AD.

ACKNOWLEDGMENTS

The authors gratefully acknowledge the Leibniz Supercomputing Centre for funding this project by providing computing time on its Linux-Cluster.

Data collection and sharing for this project were funded by the ADNI (National Institutes of Health Grant U01 AG024904) and DOD ADNI (Department of Defense Award W81XWH-12-2-0012). ADNI is funded by the National Institute on Aging and the National Institute of Biomedical Imaging and Bioengineering and through generous contributions from the following companies and organiztaions: Alzheimer's Association; Alzheimer's Drug Discovery Foundation; Araclon Biotech; BioClinica, Inc.; Biogen Idec Inc.; Bristol-Myers Squibb Company; Eisai Inc.; Elan Pharmaceuticals, Inc.; Eli Lilly and Company; EuroImmun; F. Hoffmann-La Roche Ltd and its affiliated company Genentech, Inc.; Fujirebio; GE Healthcare; IXICO Ltd.; Janssen Alzheimer Immunotherapy Research & Development, LLC.; Johnson & Johnson Pharmaceutical Research & Development LLC; Medpace, Inc.; Merck & Co., Inc.; Meso Scale Diagnostics, LLC; NeuroRx Research; Neurotrack Technologies; Novartis Pharmaceuticals Corp.; Pfizer Inc.; Piramal Imaging; Servier; Synarc Inc.; and Takeda Pharmaceutical Co. The Canadian Institutes of Health Research provides funds to support ADNI clinical sites in Canada. Private-sector contributions are facilitated by the Foundation for the National Institutes of Health (www.fnih.org). The grantee organization was the Northern California Institute for Research and Education, and the study was coordinated by the Alzheimer's Disease Cooperative Study at the University of California, San Diego. ADNI data are disseminated by the Laboratory of Neuro Imaging at the University of Southern California.

J-ADNI was supported by the following grants: Translational Research Promotion Project from the New Energy and Industrial Technology Development Organization of Japan; Research on Dementia, Health Labor Sciences Research Grant; Life Science Database Integration Project of Japan Science and Technology Agency; Research Association of Biotechnology (contributed by Astellas Pharma Inc.,

Bristol-Myers Squibb, Daiichi-Sankyo, Eisai, Eli Lilly and Co., Merck-Banyu, Mitsubishi Tanabe Pharma, Pfizer Inc., Shionogi & Co., Ltd., Sumitomo Dainippon, and Takeda Pharmaceutical Company), Japan, and a grant from an anonymous foundation.

Finally, this research was conducted using the UK Biobank Resource under Application No. 34479. This research was supported by the Bavarian State Ministry of Science and the Arts and coordinated by the Bavarian Research Institute for Digital Transformation, and the Federal Ministry of Education and Research in the call for Computational Life Sciences (DeepMentia, 031L0200A).

Open access funding enabled and organized by Projekt DEAL.

CONFLICT OF INTEREST

The authors declare no competing interests.

CODE AVAILABILITY

The code used in this study is available at https://github.com/ai-med/causal-effects-in-alzheimers-continuum.

REFERENCES

1. Pearl J. *Causality: Models, Reasoning, and Inference*. 2nd ed., Cambridge University Press; 2009.
2. Lockhart SN, DeCarli C. Structural imaging measures of brain aging. *Neuropsychol Rev*. 2014;24(3):271-289.
3. Dukart J, Schroeter ML, Mueller K. Age correction in dementia-matching to a healthy brain. *PloS One*. 2011;6(7):e22193.
4. Fortin JP, Cullen N, Sheline YI, et al. Harmonization of cortical thickness measurements across scanners and sites. *Neuroimage*. 2018;167:104-120.
5. Koikkalainen J, Pölönen H, Mattila J, van Gils M, Soininen H, Lötjönen J. Improved classification of Alzheimer's disease data via removal of nuisance variability. *PLoS One*. 2012;7(2):e31112.
6. Kostro D, Abdulkadir A, Durr A, et al. Correction of inter-scanner and within-subject variance in structural MRI based automated diagnosing. *Neuroimage*. 2014;98:405-415.
7. Neto EC. Causality-aware counterfactual confounding adjustment as an alternative to linear residualization in anticausal prediction tasks based on linear learners. *Proceedings of 38th International Conference on Machine Learning (ICML)*. 2021;139:8034-8044.
8. Snoek L, Miletić S, Scholte HS. How to control for confounds in decoding analyses of neuroimaging data. *Neuroimage*. 2019;184:741-760.
9. Yamashita A, Yahata N, Itahashi T, et al. Harmonization of resting-state functional MRI data across multiple imaging sites via the separation of site differences into sampling bias and measurement bias. *PLoS Biol*. 2019;17(4):e3000042.
10. Linn KA, Gaonkar B, Doshi J, Davatzikos C, Shinohara RT. Addressing confounding in predictive models with an application to neuroimaging. *Int J Biostat*. 2016;12(1):31-44.
11. Rao A, Monteiro JM, Mourao-Miranda J. Predictive modelling using neuroimaging data in the presence of confounds. *Neuroimage*. 2017;150:23-49.
12. Wachinger C, Rieckmann A, Pölsterl S. Detect and correct bias in multi-site neuroimaging datasets. *Med Image Anal*. 2021;67:101879.
13. Alfaro-Almagro F, McCarthy P, Afyouni S, et al. Confound modelling in UK Biobank brain imaging. *Neuroimage*. 2021;224:117002.
14. Andrews SJ, Fulton-Howard B, O'Reilly P, Marcora E, Goate AM, collaborators of the Alzheimer's Disease Genetics Consortium. Causal associations between modifiable risk factors and the Alzheimer's phenome. *Ann Neurol*. 2021;89(1):54-65.
15. Knutson KA, Deng Y, Pan W. Implicating causal brain imaging endophenotypes in Alzheimer's disease using multivariable IWAS and GWAS summary data. *NeuroImage*. 2020;223:117347.
16. Ou YN, Yang YX, Shen XN, et al. Genetically determined blood pressure, antihypertensive medications, and risk of Alzheimer's disease: a Mendelian randomization study. *Alzheimers Res Ther*. 2021;13(1):41.
17. Sproviero W, Winchester L, Newby D, et al. High blood pressure and risk of dementia: a two-sample mendelian randomization study in the UK biobank. *Biol Psychiatry*. 2021;89(8):817-824.
18. Sun YQ, Richmond RC, Chen Y, Mai XM. Mixed evidence for the relationship between periodontitis and alzheimer's disease: A bidirectional mendelian randomization study. *PLoS One*. 2020;15(1):e0228206.
19. Yeung CHC, Lau KWD, Au Yeung SL, Schooling CM. Amyloid, tau and risk of Alzheimer's disease: a Mendelian randomization study. *Eur J Epidemiol*. 2021;36(1):81-88.
20. Wu BS, Zhang YR, Li HQ, et al. Cortical structure and the risk for Alzheimer's disease: a bidirectional Mendelian randomization study. *Transl Psychiatry*. 2021;11(1):476.
21. Zhu Z, Zheng Z, Zhang F, et al. Causal associations between risk factors and common diseases inferred from GWAS summary data. *Nat Commun*. 2018;9(1):224.
22. Burgess S, Thompson SG. Multivariable Mendelian randomization: the use of pleiotropic genetic variants to estimate causal effects. *Am J Epidemiol*. 2015;181(4):251-260.
23. Smith GD, Ebrahim S. mendelian randomization: can genetic epidemiology contribute to understanding environmental determinants of disease? *Int J Epidemiol*. 2003;32(1):1-22.
24. Wang Y, Blei DM. The blessings of multiple causes. *J Am Stat Assoc*. 2019;114(528):1574-1596.
25. Ekman U, Ferreira D, Westman E. The A/T/N biomarker scheme and patterns of brain atrophy assessed in mild cognitive impairment. *Sci Rep*. 2018;8(1).
26. Jack CR, Bernstein MA, Fox NC, et al. The Alzheimer's disease neuroimaging initiative (ADNI): MRI methods. *J Magn Reson Imaging*. 2008;27(4):685-691.
27. Ihara R, Iwata A, Suzuki K, et al. Clinical and cognitive characteristics of preclinical Alzheimer's disease in the Japanese Alzheimer's Disease Neuroimaging Initiative cohort. *Alzheimer' Dement*. 2018;4(1):645-651.
28. Iwatsubo T, Iwata A, Suzuki K, et al. Japanese and north american Alzheimer's disease neuroimaging Initiative studies: harmonization for international trials. *Alzheimers Dement*. 2018;14(8):1077-1087.
29. Fischl B. FreeSurfer. *Neuroimage*. 2012;62(2):774-781.
30. Mohs RC, Knopman D, Petersen RC, et al. Development of cognitive instruments for use in clinical trials of antidementia drugs. *Alzheimer Dis Assoc Disord*. 1997;11:13-21.
31. Hedden T, Gabrieli JDE. Insights into the ageing mind: a view from cognitive neuroscience. *Nat Rev Neurosci*. 2004;5(2):87-96.
32. Barnes J, Ridgway GR, Bartlett J, et al. Head size, age and gender adjustment in MRI studies: a necessary nuisance? *Neuroimage*. 2010;53(4):1244-1255.
33. Stonnington CM, Tan G, Klöppel S, et al. Interpreting scan data acquired from multiple scanners: a study with Alzheimer's disease. *Neuroimage*. 2008;39(3):1180-1185.
34. Tipping ME, Bishop CM. Probabilistic principal component analysis. *J R Stat Soc Series B Stat Methodol*. 1999;61(3):611-622.
35. Salakhutdinov R, Mnih A. Bayesian probabilistic matrix factorization using Markov Chain Monte Carlo. *Proceedings of 25th International Conference on Machine Learning (ICML)*, 2008; 880-887.
36. Carpenter B, Gelman A, Hoffman MD, et al. Stan: a probabilistic programming language. *J Stat Softw*. 2017;76(1):1-32.
37. Ferrari S, Cribari-Neto F. Beta regression for modelling rates and proportions. *J Appl Stat*. 2004;31(7):799-815.

38. Frisoni GB, Fox NC, Jack CR, Scheltens P, Thompson PM. The clinical use of structural MRI in Alzheimer disease. *Nat Rev Neurol*. 2010;6(2):67-77.
39. Gómez-Isla T, Price JL, McKeel Jr DW, Morris JC, Growdon JH, Hyman BT. Profound loss of layer II entorhinal cortex neurons occurs in very mild Alzheimer's disease. *J Neurosci*. 1996;16(14):4491-4500.
40. Scheltens P, Leys D, Barkhof F, et al. Atrophy of medial temporal lobes on MRI in "probable" Alzheimer's disease and normal ageing: diagnostic value and neuropsychological correlates. *J Neurol Neurosurg Psychiatry*. 1992;55(10):967-972.
41. Whitwell JL, Josephs KA, Murray ME, et al. MRI correlates of neurofibrillary tangle pathology at autopsy: a voxel-based morphometry study. *Neurology*. 2008;71(10):743-749.
42. Crutch SJ, Lehmann M, Schott JM, Rabinovici GD, Rossor MN, Fox NC. Posterior cortical atrophy. *Lancet Neurol*. 2012;11(2):170-178.
43. Sun N, Mormino EC, Chen J, Sabuncu MR, Yeo BTT. Multi-modal latent factor exploration of atrophy, cognitive and tau heterogeneity in Alzheimer's disease. *Neuroimage*. 2019;201:116 043.
44. Dickerson BC, Bakkour A, Salat DH, et al. The Cortical signature of Alzheimer's disease: regionally specific cortical thinning relates to symptom severity in very mild to mild AD dementia and is detectable in asymptomatic amyloid-positive individuals. *Cereb Cortex*. 2008;19(3):497-510.
45. Su L, Surendranathan A, Huang Y, et al. Relationship between tau, neuroinflammation and atrophy in Alzheimer's disease: The NIMROD study. *Inf Fusion*. 2021;67:116-124.
46. Wei H, Kong M, Zhang C, Guan L, Ba M. The structural MRI markers and cognitive decline in prodromal Alzheimer's disease: a 2-year longitudinal study. *Quant Imaging Med Surg*. 2018;8(10):1004-1019.
47. McEvoy LK, Fennema-Notestine C, Roddey JC, et al. Alzheimer disease: Quantitative structural neuroimaging for detection and prediction of clinical and structural changes in mild cognitive impairment. *Radiology*. 2009;251(1):195-205.
48. Poulin SP, Dautoff R, Morris JC, Barrett LF, Dickerson BC. Amygdala atrophy is prominent in early Alzheimer's disease and relates to symptom severity. *Psychiatry Res Neuroimaging*. 2011;194(1):7-13.
49. Schwarz CG, Gunter JL, Wiste HJ, et al. A large-scale comparison of cortical thickness and volume methods for measuring Alzheimer's disease severity. *Neuroimage Clin*. 2016;11:802-812.
50. Cervenka S, Bäckman L, Cselényi Z, Halldin C, Farde L. Associations between dopamine D2-receptor binding and cognitive performance indicate functional compartmentalization of the human striatum. *Neuroimage* 2008;40(3):1287-1295.
51. de Jong LW, Wang Y, White LR, Yu B, van Buchem MA, Launer LJ. Ventral striatal volume is associated with cognitive decline in older people: a population based MR-study. *Neurobiol Aging*. 2012;33(2):424.e1-424.e10.
52. Yi HA, Möller C, Dieleman N, et al. Relation between subcortical grey matter atrophy and conversion from mild cognitive impairment to Alzheimer's disease. *J Neurol Neurosurg Psychiatry*. 2015;87(4):425-432.
53. Ramos Bernardes da Silva Filho S, Oliveira Barbosa JH, Rondinoni C, et al. Neuro-degeneration profile of Alzheimer's patients: a brain morphometry study. *Neuroimage Clin*. 2017;15:15-24.
54. Frederiksen KS, Garde E, Skimminge A, et al. Corpus callosum tissue loss and development of motor and global cognitive impairment: The LADIS study. *Dement Geriatr Cogn Disord*. 2011;32(4):279-286.
55. Hallam BJ, Brown WS, Ross C, et al. Regional atrophy of the corpus callosum in dementia. *Int Neuropsychol Soc*. 2008;14(03):414-423.
56. Teipel SJ, Bayer W, Alexander GE, et al. Progression of corpus callosum atrophy in Alzheimer disease. *Arch Neurol*. 2002;59(2):243-248.
57. Tomaiuolo F, Scapin M, Paola MD, et al. Gross anatomy of the corpus callosum in Alzheimer's disease: regions of degeneration and their neuropsychological correlates. 2006;23(2):96-103.
58. Augustine JR. *Human Neuroanatomy*. 2nd ed., Wiley Blackwell; 2017.
59. Suvà D, Favre I, Kraftsik R, Esteban M, Lobrinus A, Miklossy J. Primary motor cortex involvement in Alzheimer disease. *J Neuropathol Exp Neurol*. 1999;58(11):1125-1134.
60. Jawhar S, Trawicka A, Jenneckens C, Bayer TA, Wirths O. Motor deficits, neuron loss, and reduced anxiety coinciding with axonal degeneration and intraneuronal Aβ aggregation in the 5XFAD mouse model of Alzheimer's disease. *Neurobiol Aging*. 2012;33(1):196.e29-196.e40.
61. Scherder E, Eggermont L, Swaab D, et al. Gait in ageing and associated dementias; its relationship with cognition. *Neurosci Biobehav Rev*. 2007;31(4):485-497.
62. Sabuncu MR, Desikan RS, Sepulcre J, et al. The dynamics of cortical and hippocampal atrophy in Alzheimer disease. *Arch Neurol*. 2011;68(8):1040.
63. Montero-Odasso M, Pieruccini-Faria F, Bartha R, et al. Motor phenotype in neurodegenerative disorders: gait and balance platform study design protocol for the ontario neurodegenerative research initiative (ONDRI). *J Alzheimers Dis*. 2017;59(2):707-721.
64. Beckett LA, Donohue MC, Wang C, Aisen P, Harvey DJ, Saito N. The Alzheimer's Disease Neuroimaging Initiative phase 2: increasing the length, breadth, and depth of our understanding. *Alzheimers Dement*. 2015;11(7):823-831.
65. Petersen RC, Aisen PS, Beckett LA, et al. Alzheimer's disease neuroimaging initiative (ADNI): clinical characterization. *Neurology*. 2009;74(3):201-209.
66. Kang H, Zhang A, Cai TT, Small DS. Instrumental variables estimation with some invalid instruments and its application to mendelian randomization. *J Am Stat Assoc*. 2016;111(513):132-144.
67. Nelson HE, O'Connell A. Dementia: The estimation of premorbid intelligence levels using the new adult reading test. *Cortex*. 1978;14(2):234-244.
68. Cano SJ, Posner HB, Moline ML, et al. The ADAS-cog in Alzheimer's disease clinical trials: psychometric evaluation of the sum and its parts. *J Neurol Neurosurg Psychiatry*. 2010;81(12):1363-1368.
69. Pyo G, Elble RJ, Ala T, Markwell SJ. The characteristics of patients with uncertain/mild cognitive impairment on the alzheimer disease assessment scale-cognitive subscale. *Alzheimer Dis Assoc Disord*. 2006;20(1):16-22.
70. Verma N, Beretvas SN, Pascual B, Masdeu JC, Markey MK. New scoring methodology improves the sensitivity of the Alzheimer's Disease Assessment Scale-Cognitive subscale (ADAS-Cog) in clinical trials. *Alzheimers Res Ther*. 2015;7:64.
71. Jack Jr CR, Bennett DA, Blennow K, et al. NIA-AA research framework: Toward a biological definition of Alzheimer's disease. *Alzheimers Dement*. 2018;14(4):535-562.

SUPPORTING INFORMATION

Additional supporting information can be found online in the Supporting Information section at the end of this article.

How to cite this article: Pölsterl S, Wachinger C. Identification of causal effects of neuroanatomy on cognitive decline requires modeling unobserved confounders. *Alzheimer's Dement*. 2023;19:1994–2005.
https://doi.org/10.1002/alz.12825